NEXUS ENGINEERING CHRONICLE
Volume 02 Number 01 (2026)
10.5281/zenodo.18321449
https://nexusjurnal.org/ojs/index.php/nec

Article

Decarbonizing Onshore Oil and Gas Operation for EOR Using Aspen HYSYS and CMG-STARS Simulators

Asiedu Isaac[1], Charles Boakye[1*] and Prince Appiah Owusu[1]

1. Department of Oil and Gas Engineering, Kumasi Technical University, Kumasi- Ghana
* Correspondence: charlesboakye81@gmail.com

Abstract: The global pursuit of decarbonization and net-zero emissions by 2050 has positioned carbon capture, utilization, and storage (CCUS) as a critical pathway for climate mitigation. Among its approaches, CO_2-enhanced oil recovery (CO_2-EOR) offers the dual benefit of reducing atmospheric emissions while improving recovery from mature reservoirs. This research develops an integrated modeling framework that combines Aspen HYSYS surface process simulation for CO_2 capture and conditioning with CMG STARS reservoir simulation for injection performance. A post-combustion capture system using 30 wt% monoethanolamine (MEA) was modeled In the Aspen HYSYS V14.4 with absorbers, strippers, and dehydrators configured to produce pipeline-grade CO_2. Sensitivity analysis was performed on tray numbers in the absorbers, strippers, and dehydrators showing their effect on the final CO_2 purity of (≈99.67%) at 5 bar and 37 °C, confirming technical feasibility for injection. The conditioned CO_2 of (≈99.67%) purity was injected into a synthetic reservoir at 1.0 MMSCFD, for 5000days simulation period in the CMG STARS reservoir simulator, resulting cumulative oil recovery of 931,936 bbl and a recovery factor of 31.12%. Over the simulation period about 5 MMMSCF (of ~570,000 tonnes) of CO_2 was captured and sequestered avoiding equivalent atmospheric CO_2 concentration increase of ~7.3×10^{-5} ppmv and ~8.0×10^{-7} °C equilibrium global warming temperature increase. These results highlight the dual role of CO_2-EOR as both a decarbonization strategy and a production-enhancing technique.

Keywords: Carbon Capture, CO2-EOR, Onshore Oil and Gas Operation

1. Introduction

Human activities now release approximately 40 Gt of CO_2 per year equivalent to 11.1 Gt of carbon driven largely by fossil fuel combustion and industrial processes. A substantial fraction stems from onshore oil and gas operations, which alone contribute about 4.5 to 4.8 Gt CO_2-equivalent annually, accounting for nearly 14% of global energy-related emissions (Climate TRACE, 2023; IEA, 2024). [1] The atmospheric concentration of CO_2 has climbed roughly 50% above pre-industrial levels, acting as a potent greenhouse gas that traps heat and accelerates global warming [2].

Both the Intergovernmental Panel on Climate Change (IPCC, 2018) and the International Energy Agency (IEA, 2021) highlights this as an urgency which calls for global decarbonization in onshore oil and gas operations [3]. The indispensable pathway to reduce CO_2 emissions from this hard-to-abate onshore oil and gas energy sector is to a adopt to CCUS.

The impetus for decarbonizing onshore oil and gas operations stems from its environmental necessity and arising economic and regulatory pressures [4]. The primary environmental cause is the unequivocal scientific consensus [1] highlighting CO_2 emission from fossil fuel from combustion such as flaring, venting, methane leaks, and energy-intensive process as the primary causes for global warming [3]. Also, economically, shifting investors and customer preference, coupled with rising risks of high-carbon assets, alongside carbon pricing mechanisms like taxes and trading systems [2].

Citation: Isaac, A., Boakye, C., Owusa, A. Decarbonizing Onshore Oil and Gas Operation for EOR Using Aspen HYSYS and CMG-STARS Simulators. Nexus Engineering Chronicle 2026, 2 (1), 1-12.
Received: 15th Aug 2025
Revised: 11th Oct 2025
Accepted: 04th Jan 2026
Published: 20th Jan 2026

As global energy demand continues to grow, integrating sustainable practices into oil and gas operations has become a critical priority. CO_2 which is an inevitable byproduct of combustion units, refining, and gas processing, and if vented directly, contributes significantly to atmospheric emissions [5]. Advances in capture technologies now allow this CO_2 to be recovered, purified, and reinjected into depleted or mature reservoirs, achieving both environmental and economic benefits. This dual role climate mitigation and improved recovery make CO_2-EOR a central strategy in balancing energy transition with sustainable development [1], [3].

Global policies which aim at de-risk the high capital investment required for CCUS such the United State 45Q tax which credits a powerful incentive, offering up to $85 per tonne of CO2 permanently stored and $60 per tonne used for EOR [4]. Similarly, the European Union's Innovation Fund and Emissions Trading System (ETS) also create a favourable investment landscape for CCUS project.CO2-EOR offers a unique value proposition by turning a waste product (CO2) and a cost (carbon tax) into a valuable commodity that enhances production and generates revenue. Onshore CO_2 Emission Sources and Capture Technologies [6].

Carbon dioxide (CO_2) emissions in the onshore upstream and midstream oil and gas value chain arise from multiple sources, offering varied opportunities for capture based on concentration, pressure, and contaminant levels [7]. Also capture technologies, tailored to CO_2 concentration, gas pressure, temperature, and proximity to injection infrastructure, include methods with differing efficiencies, costs, and complexities, enabling targeted mitigation of these emissions.

1.1 Onshore CO_2 Emission Sources

Flue Gas from Combustion Units: Flue gas from combustion units, including gas-fired turbines, heaters, and boilers in oil and gas operations, is a significant CO_2 emission source, containing 8–14% CO_2 by volume alongside nitrogen, water vapor, oxygen, and trace pollutants, making capture challenging due to its dilute concentration and low pressure (Aaron and Tsouris, 2005; IPCC, 2006).

Gas Processing Facilities: In gas processing facilities, CO_2 content in raw natural gas can range from 10–15% and up to 20–30% in mature or sour gas fields, particularly in regions with volcanic or geothermal activity (IPCC, 2006; Rojey, 2009). This concentrated and moderately pressurized CO_2, often processed centrally, makes it an economical and attractive source for large-scale capture and reuse in CO_2-enhanced oil recovery (EOR) projects, as demonstrated by initiatives in North America (IEAGHG, 2019).

Acid Gas Removal Units: In acid gas removal units, CO_2 concentration in the separated acid gas stream can exceed 50%, often at elevated pressures of 600–1000 psi, making it a highly concentrated and energy-efficient source for capture (IEAGHG, 2019; IPCC, 2006).

Flaring Operations: Flaring operations in oil and gas fields burn associated gas, producing flue gas with 8–14% CO_2 by volume, though its intermittent nature, high temperature, and low pressure pose challenges for capture (IPCC, 2006; World Bank, 2022). Despite this, flare gas recovery units (FGRUs) and mini processing units are increasingly used to capture CO_2 for reuse in enhanced oil recovery (EOR), driven by regulatory pressures like the World Bank's Zero Routine Flaring Initiative (IEAGHG, 2019; World Bank, 2022).

CO_2 Capture Technologies.

Amine-Based Absorption: Amine absorption, the most mature CO_2 capture method for natural gas and flue gases, involves chemical reaction with solvents like MEA, DEA, or MDEA in an absorber column, followed by regeneration through heating in a stripper to release high-purity CO_2 and recycle the solvent (Kohl and Nielsen, 1997). It excels at low CO_2 partial pressures, ideal for post-combustion and low-pressure streams.

Membrane Separation: Membrane-based separation employs semipermeable polymer membranes to selectively separate CO_2 from gases like methane. It's compact, requires no chemical regeneration, and is effective for moderate CO_2 concentrations. However, its selectivity and energy efficiency decrease at lower pressures or with dilute CO_2. It's often used as a polishing step after bulk separation (Baker and Low, 2014).

Cryogenic Distillation: Cryogenic distillation cools gas streams to very low temperatures to condense or solidify CO_2 for separation from other gases. It's highly effective for high

CO_2 concentrations (above 90%) and is used in gas purification and natural gas liquefaction. However, its high energy demand makes it unsuitable for dilute CO_2 streams (Rojey, 2009).

Pressure Swing Adsorption (PSA): In PSA systems, CO_2 is adsorbed onto solid materials like zeolites or activated carbon under high pressure. When the pressure is reduced, the CO_2 is released and collected. PSA is generally applied in smaller-scale or high-purity CO_2 applications and is best suited for relatively concentrated CO_2 sources. Technology has fast cycle times but lower efficiency when treating low-concentration streams (Songolzadeh et al., 2014).

For the sake of this study flue gas from combustion units is selected for CO_2 capture due to its significant contribution to emissions in onshore oil and gas operations, despite its dilute CO_2 content (8–14%) and low pressure (Aaron and Tsouris, 2005; IPCC, 2006). Amine-based absorption is chosen for CO_2 capturing process due its high efficiency (>90%) and ability to handle low-concentration streams, as proven in projects like ADNOC and Shell's Quest CCS (Kohl and Nielsen, 1997; IEAGHG, 2019; Shell, 2020). In the process, CO_2 reacts with monoethanolamine (MEA) in the absorber:

$$CO_2 + 2RNH_2 \rightleftharpoons RNH_3^+ + RNHCOO^-$$

Forming carbamate and ammonium ions, which are later heated in the stripper to release pure CO_2 and regenerate the amine. This method ensures effective capture and compatibility with enhanced oil recovery (EOR) applications.

2. Materials and Methods

This study will adopt modeling-based research methodology that integrates surface process simulation with reservoir performance evaluation. The goal is to simulate the end-to-end utilization of captured CO_2 from onshore oil and gas operations for enhanced oil recovery (EOR). The approach combines chemical process modeling in Aspen HYSYS V1 with static reservoir modeling in CMG, using synthetic but technically realistic parameters.

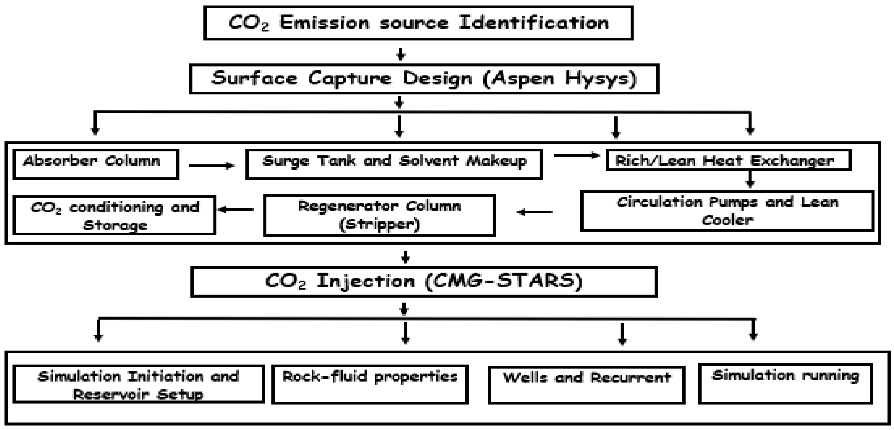

Figure 1.0. The flow chart of the surface CO2 capture to the reservoir injection

2.1. CO_2 surface Capture in Aspen HYSYS

Flue gas from combustion units, containing CO_2, nitrogen, water, H_2S, oxygen, helium, formic acid, $H_2S_2O_3$, HSCN, and hydrogen, is selected for this study, as the CO_2 source due to its prominence in onshore oil and gas emissions (Aaron and Tsouris, 2005; IPCC, 2006). A 30% wt monoethanolamine (MEA) fluid package was imported as the simulation's thermodynamic property method in the Aspen HYSYS, this package is pre-configured with parameters for optimizing acid gas absorption including temperature-dependent equilibrium constants and reaction kinetics relevant for CO_2-amine systems. The MEA is chosen for its high CO_2 reactivity, efficient regeneration, and proven commercial success in gas treatment. The simulation models a classic amine absorption-regeneration cycle, seamlessly integrating an absorber for CO_2 capture, a regenerator for thermal stripping of CO_2 from rich amine, and supporting units like heat exchangers, pumps, separation vessels and storage tank to replicate steady-state post-combustion conditions of a real-world gas plant. The figure 3.0, table 1.0. and figure 2.0. below shows the process flow diagram of the surface CO_2 capture and the initial flue components and properties respectively.

Table 1.0. Initial flue gas composition from the Combustion units

Flue gas component	Composition (Mole fraction)
CO2	0.1250
Oxygen	0.0704
Nitrogen	0.7439
H2O	0.0597
Hydrogen	0.0001
CO	0.0000
Helium	0.0008
Formic Acid	0.0000
H2S2O3	0.0000
HSCN	0.0000
H2S	0.0000

Stream Name	Flue gas	Vapour Phase
Vapour / Phase Fraction	1.0000	1.0000
Temperature [C]	38.00	38.00
Pressure [kPa]	112.0	112.0
Molar Flow [kgmole/h]	1015	1015
Mass Flow [kg/h]	3.011e+004	3.011e+004
Std Ideal Liq Vol Flow [m3/h]	52.19	52.19
Molar Enthalpy [kJ/kgmole]	-6.325e+004	-6.325e+004
Molar Entropy [kJ/kgmole-C]	5.140	5.140
Heat Flow [kJ/h]	-6.418e+007	-6.418e+007
Liq Vol Flow @Std Cond [m3/h]	7138	7138
Fluid Package	Basis-1	

Figure 2.0 Initial properties of the flue gas

2.1.1 Absorber Column Design

The absorber column, the primary unit for CO_2 removal from flue gas, facilitates counter-current contact between upward-flowing flue gas and downward-flowing lean monoethanolamine (MEA) solution to capture CO_2. A sensitivity analysis was conducted on the absorber's stage numbers/tray positions (15, 17, and 20 trays) to assess their impact on operating temperature, pressure profiles, and CO_2 purity (mole fraction). The analysis aimed to optimize mass transfer and ensure industrial-level CO_2 absorption performance under low partial pressure conditions.

2.1.2 Regenerator Column Design

The rich monoethanolamine (MEA) stream, preheated by a cross-heat exchanger, enters the regenerator column near the top, where it descends while steam from the bottom reboiler flows upward, breaking down CO_2-rich carbamate complexes to release gaseous CO_2. A sensitivity analysis evaluated stage numbers/tray positions (23, 26, and 30 trays) to determine the optimal tray configuration for sufficient vapor-liquid contact, ensuring effective CO_2 desorption and purification.

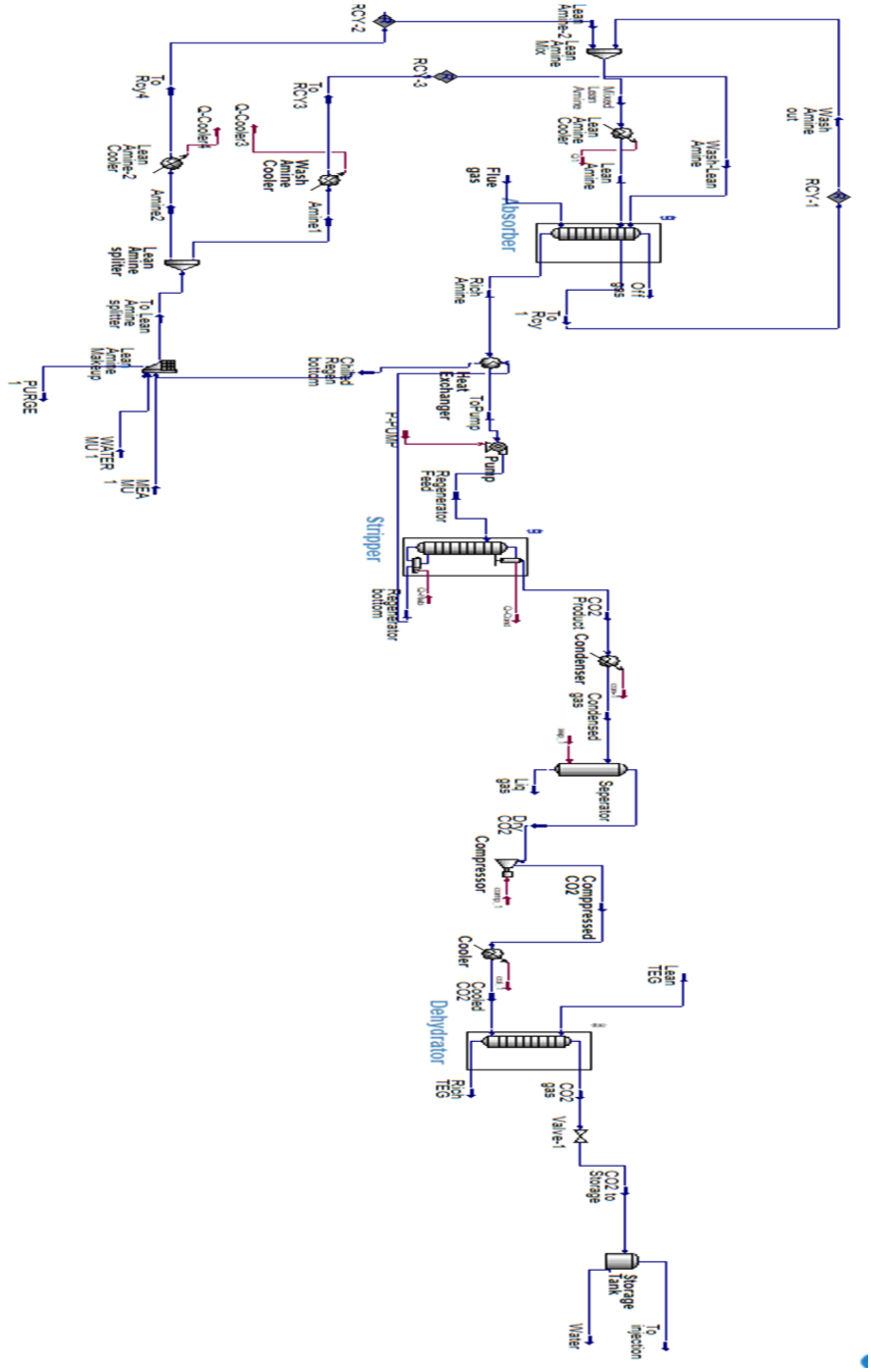

Figure 3.0. The Process Flow Diagram of the Surface CO2 capture

2.1.3 Lean/Rich Solvent Circulation and Heat Integration

In the CO_2 absorption process, thermal energy is efficiently recovered by transferring heat from the hot lean MEA stream exiting the regenerator to the cooler rich MEA stream via a Rich/Lean Cross Heat Exchanger, reducing the reboiler's energy demand and operating costs. The rich MEA, loaded with CO_2 from the absorber, is pressurized by a Rich Amine Pump before preheating and entering the regenerator for CO_2 stripping. After regeneration, the lean MEA is cooled in a Lean Amine Cooler to an optimal absorption temperature to maintain effective CO_2 capture and mass transfer efficiency in the absorber. This heat integration enhances the system's thermal efficiency and supports cost-effective operation.

2.1.4 Amine Makeup Solvent Management

The CO_2 capture process uses a 30 wt% monoethanolamine (MEA) solution, with a solvent makeup loop to counter losses from chemical degradation, evaporation, and entrainment. Fresh MEA is injected at the lean amine surge tank, located downstream of the regenerator and before the lean amine cooler, to stabilize solvent composition and inventory. This compensates for degradation in the reboiler due to high temperatures and minor entrainment losses in the absorber's overhead gas stream. The makeup loop ensures the lean amine remains at 30 wt% MEA, maintaining reactivity, thermal stability, and chemical balance for consistent CO_2 capture efficiency.

2.1.5 CO_2 Conditioning and Storage

In the Aspen HYSYS CO_2 capture simulation, the recovered CO_2 gas from the regenerator undergoes conditioning to meet purity and injection specifications. The process begins with cooling and partial condensation in a condenser to remove water vapor and heavier hydrocarbons, followed by separation in a two-phase separator to isolate the CO_2-rich vapor. The dry CO_2 is then compressed to increase its density and cooled to stabilize it for dehydration. Finally, a triethylene glycol (TEG) contactor removes residual water vapor, ensuring the CO_2 stream is ready for transportation and reservoir

Table 2. Design and operating parameters for the CO2 capture in Aspen Hysys

Equipments	Parameters
Absorber Parameters	Stage number/tray position analysis on CO_2 purity (mole fraction) 15 →0.02221 17 →0.02240 20 → 0.02241 Flue gas inlet temperature (38 °C) Absorber pressure (1.12 bar) Flue gas inlet flowrate (7138 m3/h)
Heat Exchanger	Pre-heated aqueous Rich CO_2-amine from 57°C to 80°C before entering the Pump
Pump	Increase the pressure from Heat exchanger to 1.15 bar before entering the regenerator
Stripper Parameters	Stage number/tray position analysis on CO_2 purity (mole fraction) 23 →0.96117 26 →0.96122 30 → 0.96124 Regenerator feed inlet temperature (80 °C) Absorber pressure (1.15 bar)
Compressor	Compresses the dry CO_2 from the separator to 5 bar
Cooler	Reduces the compressed CO_2 temperature from 176°C to 30°C
Dehydrator Parameters	Stage number/tray position analysis on CO_2 purity (mole fraction) 10 →0.99653 15 →0.99671 20 → 0.99672 Cooled CO_2 inlet temperature (30 °C) Absorber pressure (5 bar)
Storage Tank	Receives 38,135 m3 (~1,346,477 scf/day) from dehydrated CO2 gas Discharges 28,320 m3 (~ 1MM scf/day) for sub-surface injection

2.2. CO_2 Sub-surface Reservoir Injection Simulation in CMG

The study employs the CMG STARS module to simulate CO_2-enhanced oil recovery (EOR) in a synthetic reservoir, using a mechanistic model to represent fluid flow and displacement dynamics without complex geological data, ideal for academic or early-phase studies. The simulation evaluates the effectiveness of CO_2, captured and conditioned from oil and gas operations (via Aspen HYSYS), in enhancing oil recovery. A one-injector and one- injection. producer well configuration is used to model a typical EOR scenario, enabling clear analysis of the CO_2 displacement front, oil production trends, CO_2 sequestration potential and recovery factor over time

2.2.1. Model Preparation and Grid Setup

The CO_2-EOR simulation was initialized in CMG STARS using Field Units (psi, ft^3/day, bbl) to align with oil and gas industry standards, employing a single-porosity model for simplicity. A Cartesian grid was constructed with 20 blocks (150 ft each) in the I-direction (3,000 ft total), 9 blocks (100 ft each) in the J-direction (900 ft total), and 6 blocks (10 ft each) in the K-direction (60 ft total), a total reservoir area of 2.7 MM ft^2 balancing computational efficiency and spatial resolution.

2.2.2. Reservoir Property Input and Fluid Initialization

The CO_2-EOR simulation in CMG STARS incorporates layer-specific porosity values (ranging from 0.08 to 0.20 across six layers) to model vertical heterogeneity, influencing fluid saturation, storage, and flow behavior in a realistic reservoir environment. A uniform permeability of 200 mD is assigned in all directions, representing a moderately permeable sandstone reservoir suitable for CO_2-EOR. The fluid system includes water (density 62.4 lb/ft^3, viscosity 5 cP), dead oil (density 50 lb/ft^3, viscosity 1 cP), and CO_2, with thermodynamic properties (critical pressure, temperature, molecular weight) and physical properties (density, viscosity) defined to model multiphase interactions and CO_2 miscibility with oil. Initial conditions are set using the capillary gravity method to simulate realistic fluid distribution based on gravitational and capillary pressure balance.

2.2.3. CO_2 Injection Configuration

The CO_2-EOR simulation in CMG STARS models a linear injection-production system with two vertical wells spanning the reservoir's 3,000 ft horizontal length to evaluate fluid movement and sweep behavior. The injector well, perforated across all six reservoir layers at grid blocks 1 5 1:6, delivers 1,000,000 ft^3/day of pure CO_2 (0.9967 mole fraction) at a bottom-hole pressure (BHP) of 4,300 psi to ensure supercritical CO_2 for enhanced miscibility and mobility (Holm and Josendal, 1982; IEAGHG, 2019). The producer well, perforated at grid blocks 20 5 1:6, operates at a 2,000 psi BHP to create a pressure gradient driving CO_2 and oil flow. The simulation was run for 5,000 days (~13.7 years) to capture CO_2 propagation, oil displacement, breakthrough, and reservoir pressure evolution, aligning with industry practices for high-purity CO_2 injection (Shell, 2020).

Table 3. Reservoir, Fluid, and Well Specifications of the reservoir simulation in CMG-STARS

	Parameter	Value / Specification
Reservoir Properties	Layer 1 Porosity	0.20
	Layer 2 Porosity	0.15
	Layer 3 Porosity	0.08
	Layer 4 Porosity	0.20
	Layer 5 Porosity	0.10
	Layer 6 Porosity	0.10
	Permeability	200 mD (All direction)
Fluid Properties	Water Density	62.4 lb/ft^3
	Water Viscosity	5 cP

	Oil Density	50 lb/ft³
	Oil Viscosity	1 cP
Injector Well	Injection Rate	1,000,000 scf/day
	BHP Constraint	4,300 psi
	Perforation Interval	Grid blocks 1 5 1:6
	Injected Fluid	Pure CO_2 (mole fraction 0.9967)
Producer Well	BHP Constraint	2,000 psi
	Perforation Interval	Grid blocks 20 5 1:6

3. Results and Discussion

This chapter presents the results obtained from the integrated simulation workflow that combines surface CO_2 capture and conditioning (Aspen HYSYS) with subsurface injection and enhanced oil recovery (CMG STARS). The outcomes are discussed in detail to demonstrate how capture efficiency, gas conditioning, and injection parameters influence reservoir behavior, oil recovery, and overall system performance.

3.1. Surface CO_2 Capture

The discussion begins with the surface capture model, where flue gas treatment, absorption–regeneration, dehydration, compression, storage, and sensitivity analysis of the tray positions in the absorber, stripper, and dehydrator were simulated to produce a high-purity CO_2 stream suitable for injection.

3.1.1 Sensitivity Analysis of Stage Number Variations on CO_2 Purification

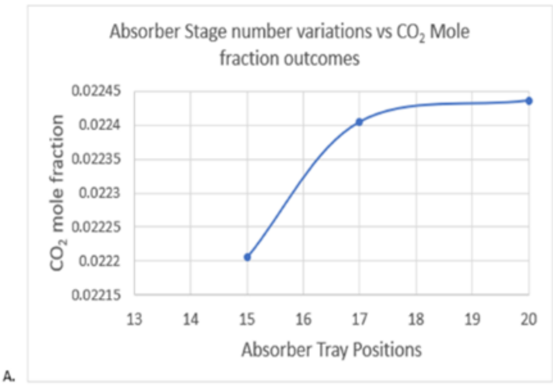

Figure 4.0. Absorber Stage number variations vs CO_2 Mole fraction outcomes.

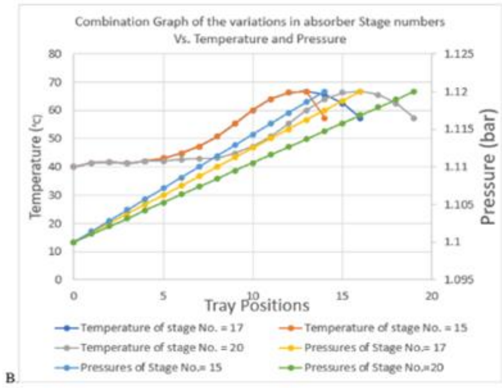

Figure 5.0. Combination Graph of the variation in absorber Stage numbers vs Temperature and Pressure

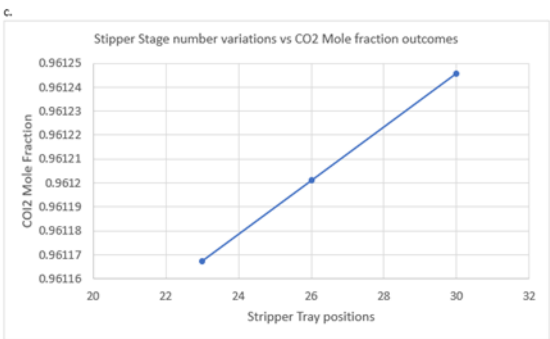

Figure 6.0. Stripper Stage number variations vs CO_2 Mole fraction outcomes

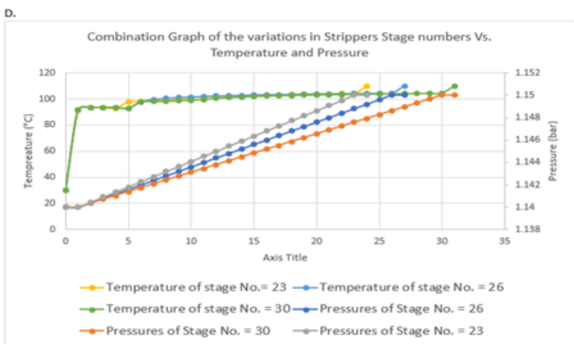

Figure 7.0. Combination Graph of the variation in Strippers Stage numbers vs Temperature and Pressure

E.

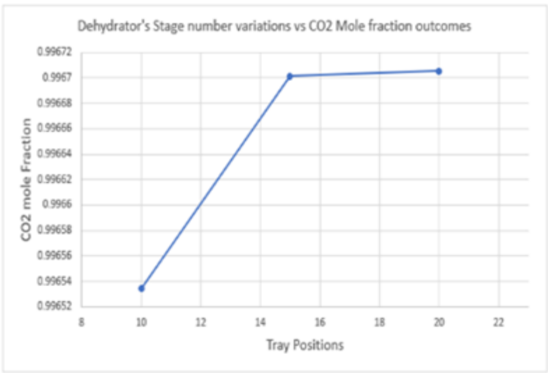

Figure 8.0. Dehydration Stage number variations vs CO_2 Mole fraction outcomes

F.

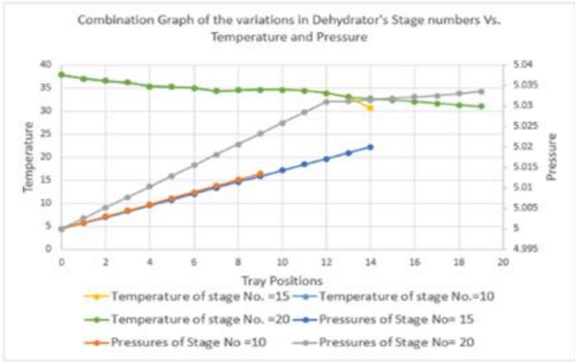

Figure 9.0. Combination Graph of the variation in Dehydration's Stage numbers vs Temperature and Pressure

A sensitivity analysis [23] in the Aspen HYSYS model evaluated tray numbers in the absorber (15, 17, 20), stripper (23, 26, 30), and dehydrator (10, 15, 20) to assess their impact on temperature, pressure, and CO_2 purity (mole fraction). In the absorber, increasing trays from 15 to 20 slightly raised CO_2 purity from 0.0222 to 0.0224 (Figure 4.0), with temperatures rising from 40–66°C and pressures slightly increasing (Figure 5), enhancing gas-liquid contact. The stripper saw CO_2 purity improve from 0.9612 to 0.96125 with more trays (Figure 6), with temperatures stabilizing at 93–104°C and pressures at 1.14–1.15 bar (Figure 7), improving solvent regeneration. The dehydrator's purity increased from 0.9965 to 0.9967 with additional trays (Figure 8), with temperatures rising from 30–37°C and pressures steady at 5 bar (Figure 9), boosting water removal efficiency. Optimal tray numbers were set at 17 for the absorber, 26 for the stripper, and 15 for the dehydrator (Figure 10), balancing high CO_2 purity (up to 99.67%) with energy efficiency and cost.

G.

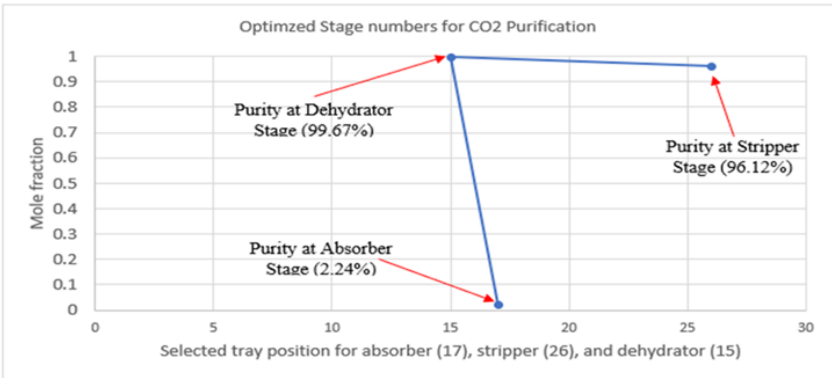

Figure 10. Optimized Stage numbers for Absorber, Stripper, and Dehydrator for CO_2 Purification

After achieving this purity through conditioning, the CO_2 is temporarily stored in a surface storage tank, receiving 38,135 m^3 (~1,346,477 scf/day) from dehydrated CO_2 gas and discharging 28,320 m^3 (~1MM scf/day) for subsurface injection.

3.2.0. CO_2 Sub-surface Injection

The reservoir simulation results detail initialization, well configuration, and the dynamic response to CO_2 injection, evaluating key metrics like cumulative oil production, recovery factor, CO_2 storage potential and performance, and sweep efficiency to gauge the injection strategy's effectiveness. Analysis was performed on the cumulative oil production with water flooding versus CO_2 flooding to determine if water would have yielded higher oil production. By integrating surface and subsurface models, the study offers a comprehensive assessment of the CO_2-EOR process, connecting process engineering with reservoir performance.

3.2.1. Reservoir Simulation Results

The CMG STARS simulation generated detailed volumetric and production data, revealing a gross formation volume of 2.89×10^7 bbl and a pore volume of 3.99×10^6 bbl, with initial aqueous and oleic phases at 9.99×10^5 bbl and 2.99×10^6 bbl respectively, indicating an oil-rich reservoir with minimal water content and no significant gas cap. The results viewer provided graphical insights into key performance indicators, including cumulative oil production, oil recovery factor, sweep efficiency via 3D saturation maps, CO_2 storage potential, and a comparative analysis of cumulative production between water and CO_2 flooding as shown below;

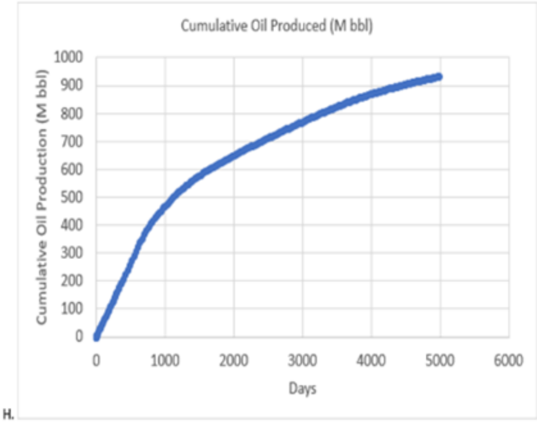

Figure 11. Cummulative Oil Production vs. Time

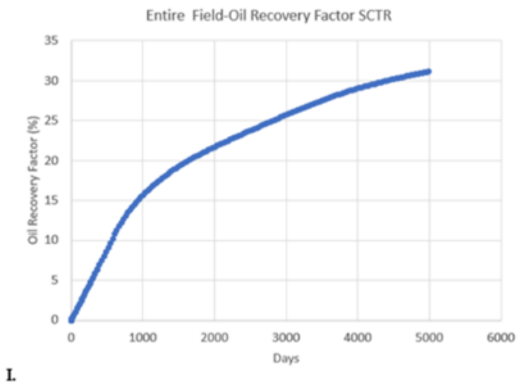

Figure 12. Recovery Factor vs. Time

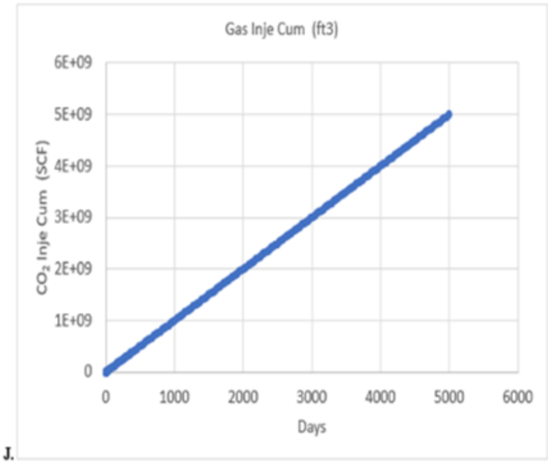

Figure 13. CO_2 Storage Performance

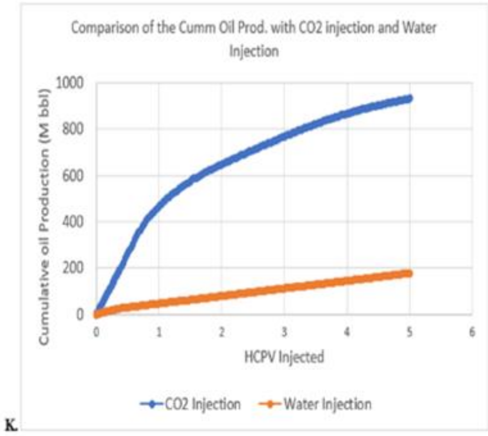

Figure 14. Comparison of the Cummulative oil production by CO_2 and water injection against HCPV

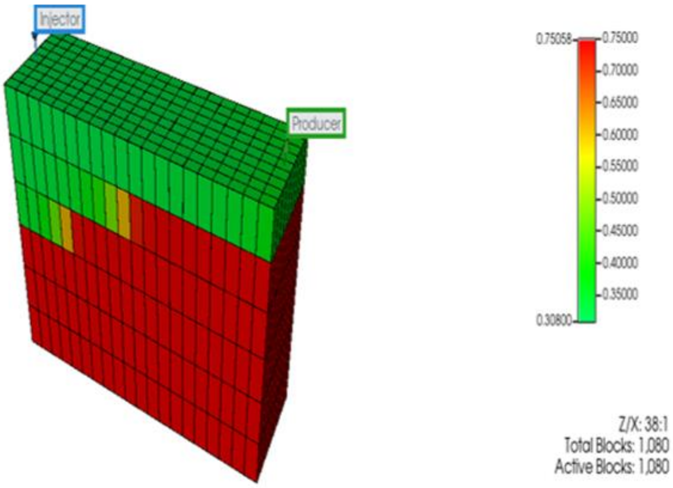

Figure 15. Sweep Efficiency Visualization in the Reservoir

The CMG STARS simulation tracked cumulative oil production, reaching 931,936 bbl over 5,000 days (Figure 11), with a recovery factor rising to 31.12% by the end (Figure 12), reflecting effective CO_2 displacement despite a plateau after 3,500 days due to breakthrough and pressure decline. CO_2 injection maintained a steady 5,000,000,000 scf over the period at 1,000,000 scf/day (Figure 13), ensuring consistent reservoir pressure and storage capacity. Compared to water injection, CO_2 flooding recovered 932,000 bbl versus 180,000 bbl (Figure 14), showcasing superior displacement due to miscibility effects, though sweep efficiency visualized in 3D (Figure 15) revealed early channeling after 4,000 days, explaining reduced incremental gains.

3.2.2. CO_2 Sequestration Potential and Climate Impact

The CMG STARS simulation quantifies the dual benefits of CO_2-EOR, sequestering 570,000 tonnes of CO_2 over 5,000 days at an injection rate of 1,000,000 scf/day (114 tonnes/day), equivalent to the annual emissions of ~120,000 cars (EPA, 2022), enhancing oil recovery (931,936 bbl) while supporting decarbonization, as seen in projects like Shell's Quest and Permian Basin initiatives. The carbon equivalent is calculated as;

$$570{,}000\ \mathrm{tCO_2} \times 0.2727 = 155{,}455\ \mathrm{tC} \approx 0.000155\ \mathrm{GtC},$$

Translating to an avoided atmospheric CO_2 increase of;

$$\Delta \mathrm{CO_2} = \frac{0.000155\ \mathrm{GtC}}{(2.13\ \mathrm{GtC/ppmv})} \approx 7.3 \times 10^{-5}\ \mathrm{ppmv}$$

This yields a radiative forcing of;

$$\Delta \mathrm{F} = 5.35 \times \frac{(7.3 \times 10^{-5})}{420} \approx 9.3 \times 10^{-7}\ \mathrm{W/m^2}$$

With an avoided temperature rise of;

$$\Delta \mathrm{T} = 0.864 \times 9.3 \times 10^{-7} \approx 8.0 \times 10^{-7}\ ^\circ\mathrm{C}$$

Indicating a minor global impact but notable contribution to regional carbon management.

Conclusion

This study validates the technical feasibility of integrating CO_2 capture with enhanced oil recovery (EOR) using Aspen HYSYS to upgrade flue gas CO_2 from 12.5% to 99.67% purity through absorption, stripping, and dehydration, with tray temperature profiles confirming efficient mass transfer and solvent regeneration. The CMG STARS simulation, injecting 1,000,000 scf/d of CO_2, yielded 931,936 bbl of oil (31.12% recovery factor) and sequestered 570,000 tonnes of CO_2 over 5,000 days, avoiding a 7.3×10^{-5} ppmv CO_2 increase and 8×10^{-7} °C warming, consistent with projects like Quest CCS and Permian Basin initiatives. This scalable, dual-purpose approach supports oil recovery and decarbonization, offering a replicable framework for net-zero goals, though further research is required. Future work should include techno-economic analysis, dynamic reservoir modeling with geological heterogeneities, long-term CO_2 storage security assessments, and sensitivity analyses on HYSYS parameters to enhance the technical, environmental, and economic viability of CO_2-EOR systems for large-scale use.

REFERENCES

[1] Aaron, D., & Tsouris, C. (2005). Separation of CO_2 from flue gas: A review. Separation Science and Technology, 40(1-3), 321–348.

[2] Baker, R. W., & Low, B. T. (2014). Gas separation membrane materials: A perspective. Macromolecules, 47(20), 6999–7013.

[3] Climate TRACE. (2023). Global emissions from oil and gas operations. https://climatetrace.org/

Global CCS Institute. (2021). Status of carbon capture and storage incentives: The 45Q tax credit. https://www.globalccsinstitute.com/resources/publications-reports-research/

[4] Holm, L. W., & Josendal, V. A. (1982). Effect of oil composition on miscible-type displacement by carbon dioxide. SPE Journal, 22(1), 87–98.

[5] IEA. (2021). Net zero by 2050: A roadmap for the global energy sector. International Energy Agency. https://www.iea.org/reports/net-zero-by-2050

[6] IEA. (2024). CO_2 emissions in 2023. International Energy Agency. https://www.iea.org/reports/co2-emissions-in-2023

[7] Najar, N. A., Najar, I. A., Bhawani, S. A., Najar, F. A., & Najar, F. A. (2025). An Overview of Mechanized Solutions for Oil Spill Treatment. Biobased Materials and Their Composites for Oil Spill Treatment, 19-38.

[8] IEAGHG. (2019). Techno-economic evaluation of CO_2 capture in LNG plants. IEAGHG Technical Report 2019-07. https://ieaghg.org/publications/technical-reports/reports-list/9-technical-reports/943-2019-07-techno-economic-evaluation-of-co2-capture-in-lng-plants-projects

[9] IPCC. (2006). 2006 IPCC guidelines for national greenhouse gas inventories. Intergovernmental Panel on Climate Change. https://www.ipcc-nggip.iges.or.jp/public/2006gl/

[10] IPCC. (2018). Global warming of 1.5°C: An IPCC special report. Intergovernmental Panel on Climate Change. https://www.ipcc.ch/sr15/

[11] Najar, I.A., Ahmadi, R., Bhawani, S.A., Namakka, M. and Ramli, N.H., 2025. Impacts of Oil Spill on Geotechnical Properties of Soil. In Biobased Materials and Their Composites for Oil Spill Treatment (pp. 39-51). Singapore: Springer Nature Singapore.

[12] IPCC. (2022). Climate change 2022: Impacts, adaptation, and vulnerability. Contribution of Working Group II to the Sixth Assessment Report of the Intergovernmental Panel on Climate Change. https://www.ipcc.ch/report/ar6/wg2/

Kohl, A. L., & Nielsen, R. B. (1997). Gas purification (5th ed.). Gulf Publishing Company. https://doi.org/10.1016/B978-0-88415-220-0.X5000-5

[13] Kokal, S., & Al-Kaabi, A. (2010). Enhanced oil recovery: Challenges & opportunities. Society of Petroleum Engineers.

[14] Morbee, J., Serres, A., & Serkin, J. (2021). Carbon pricing mechanisms: A global overview. OECD Environment Policy Papers.

[15] Moritis, G. (2012). 2012 worldwide EOR survey. Oil & Gas Journal, 110(4). http://www.ogj.com/articles/print/vol-110/issue-4/general-interest/special-report-eor-heavy-oil-survey/2012-worldwide-eor-survey.html

[16] Myhre, G., Highwood, E. J., Shine, K. P., & Stordal, F. (1998). New estimates of radiative forcing due to well mixed greenhouse gases. Geophysical Research Letters, 25(14), 2715–2718. https://doi.org/10.1029/98GL01908

[17] Najar, I.A., Bhawani, S.A., Bhat, A.H., Ahmadi, R., Tang, S., Khalik, Y.K.A. and Najar, N.A., 2025. Biodegradable Waste Sorbents for Oil Spill Treatment. In Biobased Materials and Their Composites for Oil Spill Treatment (pp. 77-90). Singapore: Springer Nature Singapore.

[18] Rojey, A., Jaffret, C., Cornot-Gandolphe, S., Durand, B., Jullian, S., & Valais, M. (2009). Natural gas production, processing, transport (Revised ed.). Editions Technip. (Original work published 1997)

[19] Shell. (2020). Quest CCS facility captures and stores five million tonnes of CO_2 ahead of fifth anniversary. https://www.shell.ca/en_ca/media/news-and-media-releases/news-releases-2020/quest-ccs-facility-captures-and-stores-five-million-tonnes.html

[20] Ben, S.K., Ahmadi, R., Bustami, R.A. and Najar, I.A., 2023, March. Numerical investigation of seismic hazard and risk of Murum Hydro-Electric Dam (MHEP). In International Conference on Dam Safety Management and Engineering (pp. 855-869). Singapore: Springer Nature Singapore.

[21] Songolzadeh, R., Soleimani, M., Takht Ravanchi, M., & Ghasemzadeh, R. (2014). Carbon dioxide separation and capture by adsorption: A review. Environmental Chemistry Letters, 12(3), 279–296.

[22]World Bank. (2022). Global gas flaring tracker report 2022. https://www.worldbank.org/en/programs/gasflaringreduction/global-flaring-data
[23] Najar, N.A., Jana, A., & Parthasarathy, D. (2025). Addressing climatic uncertainty through fleet optimization for robust winter road maintenance policy design. *Journal of Policy Modeling*. https://doi.org/10.1016/j.jpolmod.2024.12.001